# Experimentally observed phenomena on cardiac energetics in heart failure emerge from simulations of cardiac metabolism

Fan Wu[a], Jianyi Zhang[b], and Daniel A. Beard[a,1]

[a]Biotechnology and Bioengineering Center and Department of Physiology, Medical College of Wisconsin, Milwaukee, WI 53226; and [b]Cardiology Division, Department of Medicine, University of Minnesota Medical School, Minneapolis, MN 55455

Edited by Charles S. Peskin, New York University, and approved March 10, 2009 (received for review December 16, 2008)

**The failing heart is hypothesized to suffer from energy supply inadequate for supporting normal cardiac function. We analyzed data from a canine left ventricular hypertrophy model to determine how the energy state evolves because of changes in key metabolic pools. Our findings—confirmed by in vivo $^{31}$P-magnetic resonance spectroscopy—indicate that the transition between the clinically observed early compensatory phase and heart failure and the critical point at which the transition occurs are emergent properties of cardiac energy metabolism. Specifically, analysis reveals a phenomenon in which low and moderate reductions in metabolite pools have no major negative impact on oxidative capacity, whereas reductions beyond a critical tipping point lead to a severely compromised energy state. The transition point corresponds to reductions in the total adenine nucleotide pool (TAN) of ≈30%, corresponding to the reduction observed in humans in heart failure [Ingwall JS, Weiss RG (2004) Is the failing heart energy starved? On using chemical energy to support cardiac function. *Circ Res* 95(2):135–145]. At given values of TAN and the total exchangeable phosphate pool during hypertrophic remodeling, the creatine pool attains a value that is associated with optimal ATP hydrolysis potential. Thus, both increases and decreases to the creatine pool are predicted to result in diminished energetic state unless accompanied by appropriate simultaneous changes in the other pools.**

computational biology | hypertrophy | mitochondria | energy metabolism

The mechanistic relationship between energy metabolism and cardiac contractility during the development of heart failure has long eluded understanding. Observations on failing hearts show that basal ATP and phosphocreatine (CrP), as well as the total creatine pool ($CR_{tot}$), decrease steadily as cardiac hypertrophic remodeling progresses. These decreases are associated with abnormal levels of other energy metabolites in both animals and humans with left ventricular hypertrophy (LVH) and congestive heart failure (CHF), implying abnormal regulation of oxidative phosphorylation in LVH and CHF. The central hypothesis that has emerged from these observations is that the evolution from the normal to failing heart involves ''energy starvation,'' in which the ability of mitochondria to synthesize ATP at the rate and free energy required for normal cardiac function is impaired.

To understand the observed phenomena, we applied a validated computer model that simulates cellular oxygen consumption and cardiac energy metabolism. The predictions of this model challenged the widely accepted hypothesis (1) that biochemical feedback cannot explain how phosphate metabolite concentrations vary with cardiac work rate in the heart and show that the in vivo data are consistent with a critical role of inorganic phosphate (Pi) concentration as a feedback signal (2). Here we use the same model to analyze data on the evolution of LVH and CHF in a canine model. The model is adapted to LVH by varying 3 biochemical pools, the total adenine nucleotide pool (TAN), $CR_{tot}$, and the total exchangeable phosphate pool (TEP), to match data from tissue biopsy and in vivo $^{31}$P-magnetic resonance spectroscopy ($^{31}$P-MRS). These pool variables are measured in units of total mass per unit cell volume and are mathematically defined in the *Materials and Methods*. Although drastic remodeling of biochemical pathways occurs during LVH (3–5), our analysis is based on the powerful and simplifying model assumption that myocardial density, composition, and enzyme activities in the LVH heart are unchanged in comparison with the normal heart. This allows us to determine which aspects of metabolic remodeling can be explained only by the quantified changes in metabolic pools and to generate and test hypotheses on the causes and consequences of metabolic remodeling.

## Results and Discussion

**Impact of Changes in Metabolic Pools on Cardiac Energy Status.** The first step in our analysis is to determine whether the changes in metabolic pools are sufficient to explain observed data on cardiac energy state in LVH remodeling. Changes in $CR_{tot}$ and baseline CrP and ATP from $^{31}$P-MRS and biopsy measurements from a canine LVH heart model (6, 7) for early- and moderate-stage LVH are summarized in *SI Appendix*, Table S1. These experimental measurements allow us to determine the pools of $CR_{tot}$, TEP, and TAN, which are listed in the table and used to make model predictions on the relationship between rate of cardiac oxygen consumption and cellular metabolite concentrations. Fig. 1 *A–F* shows data and model predictions on steady-state CrP/ATP ratio and ΔPi/CrP ratio as functions of cardiac work rate in normal (*A* and *B*), early-stage LVH (*C* and *D*), and moderate LVH (*E* and *F*) hearts. The variable ΔPi is defined as the increase in the phosphate signal from baseline, at which the Pi concentration is too low to be measured; ΔPi/CrP is the phosphate signal measured relative to the CrP signal. The shaded data points in Fig. 1*B* correspond to the cases in which Pi falls below the limit of detection, which is ≈1 mM (6). The range of ΔPi/CrP indicated by the error bars for those data points corresponds to the range of zero to the limit of detection.

The model predictions, which involve no additional parameter adjustment, agree well with the experimental observations, indicating that the model is able to capture the in vivo relationship between work rate and phosphate metabolite concentrations observed in these experiments. Near maximal cardiac work rates, the models predict that ΔPi/CrP decreases from ≈0.16 in the normal case to ≈0.12 in the moderate LVH case, whereas the corresponding predicted free cytoplasmic Pi concentrations are

Author contributions: F.W., J.Z., and D.A.B. designed research; F.W. performed research; F.W. analyzed data; and F.W. and D.A.B. wrote the paper.

The authors declare no conflict of interest.

This article is a PNAS Direct Submission.

Freely available online through the PNAS open access option.

[1]To whom correspondence should be addressed. E-mail: dbeard@mcw.edu.

This article contains supporting information online at www.pnas.org/cgi/content/full/0812768106/DCSupplemental.

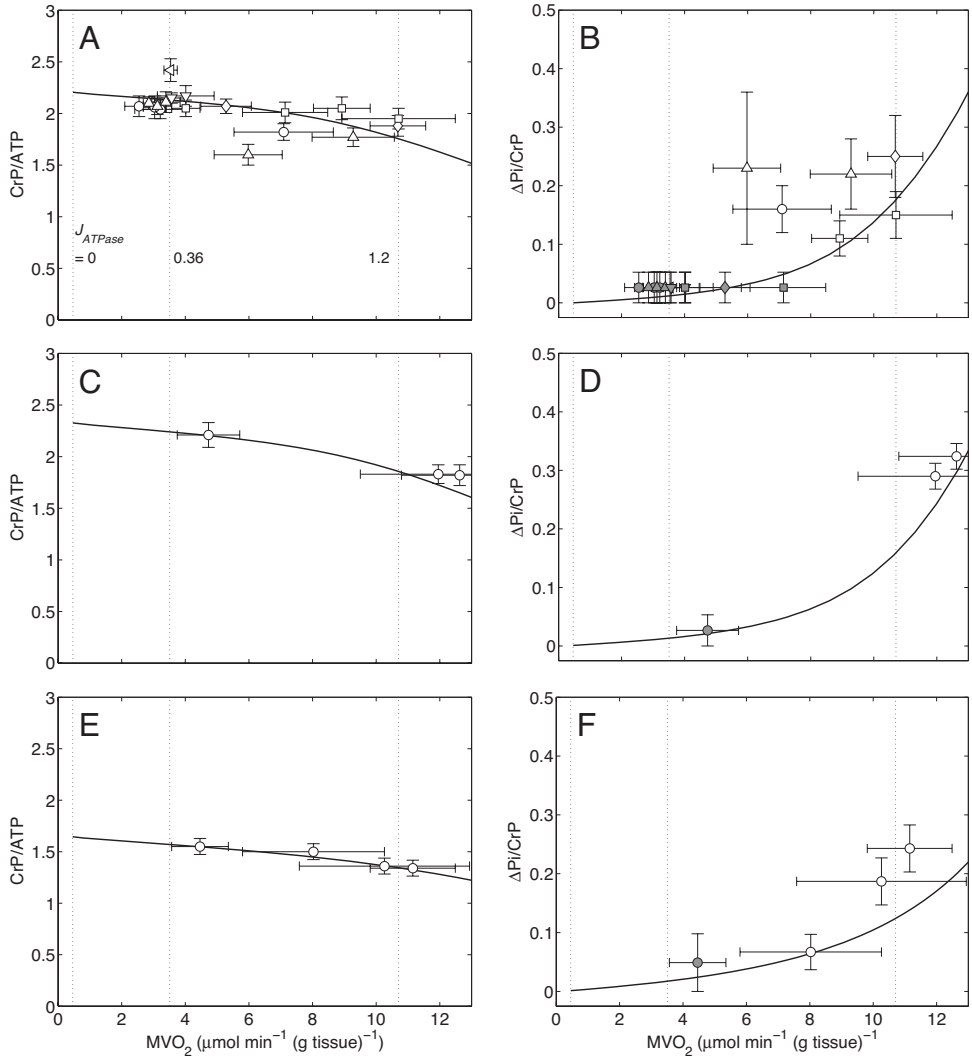


**Fig. 1.** Steady-state energetics phosphate metabolites as functions of myocardial oxygen consumption in normal and LVH hearts. Simulations are plotted as solid curves in *A* and *B* for the normal heart, *C* and *D* for the early-stage LVH heart, and *E* and *F* for the moderate LVH heart. Steady-state CrP/ATP level is plotted as a function of oxygen consumption rate, $MVO_2$, and compared with experimental data from the normal (*A*), early-stage LVH (*C*), and moderate LVH (*E*) canine heart in vivo. Steady-state ΔPi/CrP plotted as a function of $MVO_2$ and compared with experimental data from the normal (*B*), early-stage LVH (*D*), and moderate LVH (*F*) canine heart in vivo. For model predictions, $MVO_2$ is varied by varying the rate of ATP hydrolysis, $J_{ATPase}$, in the cytoplasm. The model for the normal control case (*A* and *B*) is described in Wu et al. (2). Experimental data shown in *A* and *B* are obtained from the following sources: open circles, Zhang et al. (21) (dobutamine + dopamine); open left-facing triangles, Zhang et al. (22); open diamonds, Gong et al. (16) (dobutamine + dopamine); open triangles, Ochiai et al. (23) (dobutamine + dopamine); open inverted triangles, Gong et al. (24); squares, Bache et al. (6) (dobutamine, dobutamine + dopamine). The experimental data for the early-stage and moderate LVH hearts are plotted as open circles and obtained from refs. 7 and 6, respectively. Here protocols used to elevate work load from baseline are indicated in parentheses. The values of $J_{ATPase}$ corresponding to baseline and maximal $MVO_2$, 0.36 and 1.2 mmol s$^{-1}$ (l cell)$^{-1}$, respectively, are indicated in *A*. Error bars indicate standard error.

≈2.4 and ≈1.0 mM, respectively. Given the noise and variability in the experimental data, the predicted small decrease in ΔPi/CrP from the early to the moderate case is not independently validated by the data. However, even if ΔPi/CrP is the same for these 2 cases, the significant drop in CrP shows that Pi concentration decreases from the early to the moderate case. The lower cytoplasmic Pi levels arise from a reduction of TEP compared with normal. Despite significantly altered phosphate metabolite levels, the moderate LVH heart is capable of achieving rates of ATP hydrolysis and oxygen consumption similar to the normal case.

The next step in our analysis is to determine whether and how a progressive decrease in these metabolic pools may lead to and explain a critical transition from compensatory metabolic remodeling to a noncompensatory phase in heart failure. On the basis of the findings of Zhang et al. (8) that CrP/ATP decreases in proportion to the severity of LVH indicated by the ratio of left ventricle weight to body weight (LVW/BW; see Fig. 2*A*), that $CR_{tot}$ decreases from 35.04 mmol (l cell)$^{-1}$ in normal hearts (with LVW/BW = 4.3 g kg$^{-1}$) to 27.08 mmol (l cell)$^{-1}$ in LVH hearts (with LVW/BW = 8.9 g kg$^{-1}$), and that basal ATP content decreases from 7.23 mmol (l cell)$^{-1}$ in normal hearts to 4.45 mmol (l cell)$^{-1}$ in LVH hearts, we assume linear relationships between $CR_{tot}$ and LVW/BW and between basal ATP and LVW/BW. This assumption, combined with the individual measurements on basal CrP/ATP plotted in Fig. 2*A*, allows us to estimate the values of all 3 metabolic pools for each individual case plotted in the figure. With the pool sizes estimated, we are able to use our model to predict the free energy of ATP hydrolysis ($\Delta G_{ATPase}$) at maximal work rate for these hearts, plotted in Fig. 2*B*.

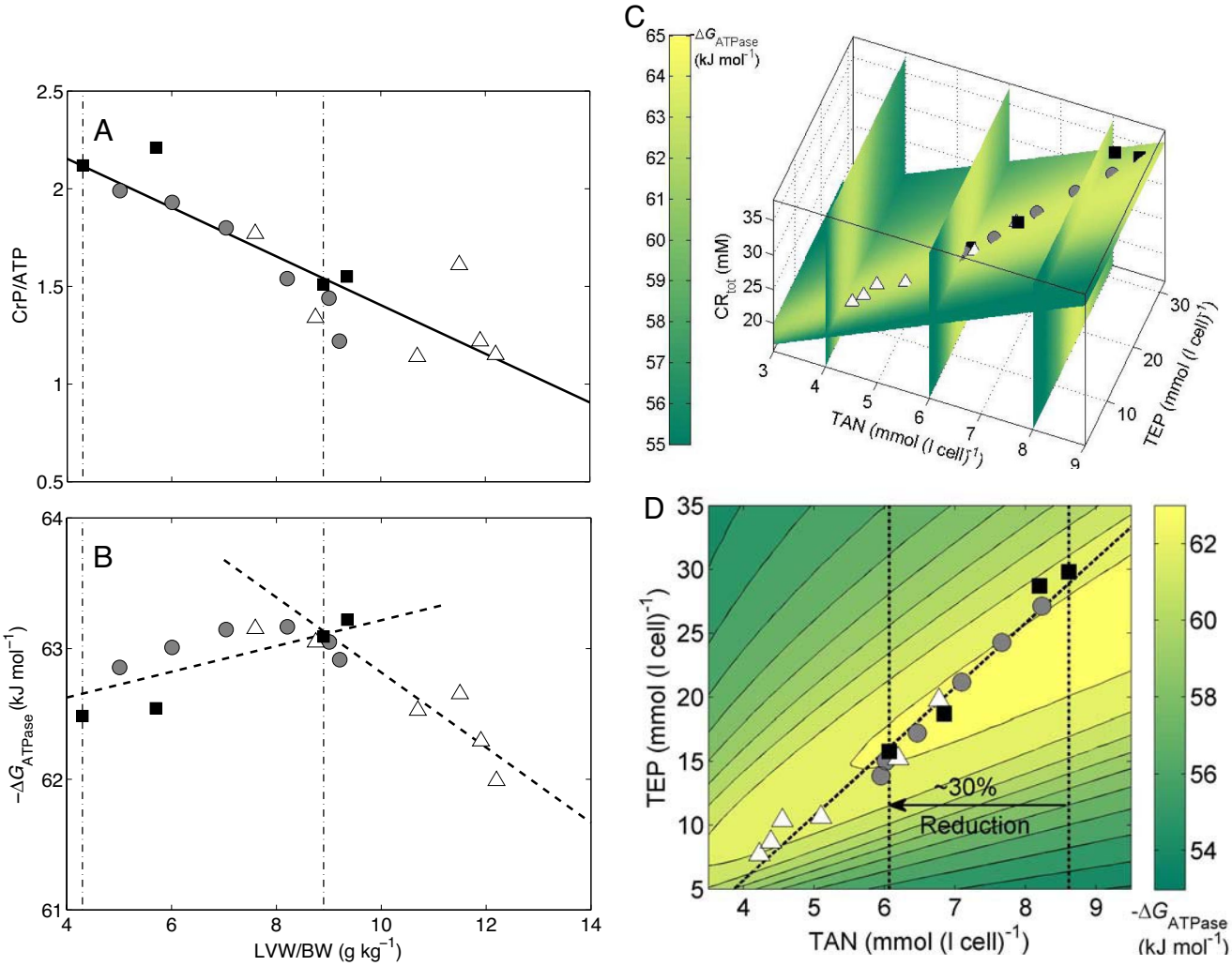


**Fig. 2.** Cardiac energetics during evolution of LVH. (*A*) Measured CrP/ATP is plotted as against LVW/BW ratio. The solid squares denote mean data measured from multiple hearts: from left to right, sources are Wu et al. (2), Bache et al. (7) (early-stage LVH), and Zhang et al. (8) and Bache et al. (6) (moderate LVH). Experimental data from individual hearts [Zhang et al. (8)] are represented as shadowed circles (with left ventricle diastolic pressure <15 mmHg) and open triangles (with left ventricle diastolic pressure >15 mmHg). The solid line is used to illustrate the linear relationship between CrP/ATP and the LVH severity (LVW/BW). The left vertical dot-dash line represents the control heart, and the right vertical dot-dash line represents the critical point where the sharp transition of energetic state takes place. (*B*) The model-predicted $\Delta G_{ATPase}$ at the maximal $MVO_2$ is plotted for the data points with symbols in *A*. The dashed lines represent the linear fit of model prediction in the 2 distinct phases of remodeling. (*C*) The model-predicted profiles of $\Delta G_{ATPase}$ at the maximal $MVO_2$ are visualized in a 3-dimensional space of $CR_{tot}$, TEP, and TAN. The model predictions in B are plotted as the same symbols in *C*. (*D*) The model-predicted profiles of $\Delta G_{ATPase}$ at the maximal $MVO_2$ are shown on a 2-dimensional plane defined by a linear relationship between $CR_{tot}$ and other pools. For each point on the surface, $CR_{tot}$ is assumed to be proportional to LVH severity and thus TAN. The dashed line represents the evolution path to heart failure.

Specifically, to make the model predictions illustrated in Fig. 2*B*, we simulate the model setting the metabolic pools at the experimentally determined values to determine $\Delta G_{ATPase}$ at maximal myocardial oxygen consumption ($MVO_2$). This analysis predicts that gradual monotonic decrease in metabolic pools is associated with the emergence of 2 distinct phases in evolution of cardiac energetic state. In early (compensatory) remodeling, maximal-work $\Delta G_{ATPase}$ is maintained or possibly increases in magnitude. A critical transition occurs around LVW/BW = 9 g kg$^{-1}$, associated with TAN, $CR_{tot}$, and TEP at ≈70%, ≈77%, and ≈53% of their normal values, respectively. When hypertrophic remodeling proceeds further and these pools are lowered beyond this critical point, the magnitude of the $\Delta G_{ATPase}$ begins to drop.

This critical transition point is associated with functional changes in cardiac contractility: all LVH hearts with left ventricular end diastolic pressure (LVEDP) <15 mmHg occur in the predicted compensatory phase or at the critical point; 4 of 6 hearts showing LVEDP >15 mmHg are predicted to be in the later failure stage. All individuals with LVEDP >15 mmHg had documented signs of clinical heart failure, including increased heart and breathing rates, decreased appetite, and refusal to exercise on the treadmill.

Clinical observations reveal that "[ATP] is 25% to 30% lower in the failing human heart," whereas "why [ATP] decreases by only 25% is not known." (3). Thus our prediction that this transition point occurs at TAN of ≈70% of normal is intriguing and potentially explains this observation. Fig. 2*C* illustrates how maximal-work $\Delta G_{ATPase}$ is predicted to vary with TAN, $CR_{tot}$, and TEP. It is observed that the individual data points from the Zhang et al. LVH model (8) approximately fall on an intersection plane illustrated in the figure. Fig. 2*D* shows a contour plot of $\Delta G_{ATPase}$ as a function of TAN and TEP on this plane. We can see that as these pools are reduced from normal [TAN = 8.62

mmol (l cell)$^{-1}$ and TEP = 29.78 mmol (l cell)$^{-1}$], $\Delta G_{ATPase}$ varies near a constant contour. Once a level of TAN ≈6.1 mmol (l cell)$^{-1}$ is reached, it is no longer possible to exceed or maintain normal basal $\Delta G_{ATPase}$. Further reductions in TAN and TEP are predicted to result in drastic reduction in ATP hydrolysis potential and impairment of cardiac function.

The association of reductions of TAN and $CR_{tot}$ with loss of cardiac function in LVH is widely acknowledged, although the causal relationship between these pools and the reduction in free energy at which cardiac mitochondria synthesize ATP has not been previously demonstrated. The importance of the TEP pool has not been previously demonstrated.

Additional related phenomena that are not included in our simulations may also contribute to changes in the energetic state during hypertrophic remodeling and heart failure. For example, experimental and clinical observations reveal significantly reduced creatine kinase (CK) activity and flux in a porcine CHF model and human failing hearts (9–12). If the CK activity is decreased to a low enough level that the CK reaction moves away from equilibrium, then the energy-buffering roles of CK would be impaired, and consequently the energetic state would worsen further. Hence reduced CK activity may exacerbate the observed distinct energy states in the early LVH stage and late CHF stage.

**Potential for Metabolic Therapy in Heart Failure.** Restoration of a normal energy state may help reverse the apoptotic process in the failing heart and prevent the further loss of function in heart failure (13). Current energy therapies rely on reduction of energy use (ATP hydrolysis rate) by limiting the workload of heart via drugs such as $\beta$-receptor blockers and angiotensin-converting enzyme inhibitors (3, 5). Observations on metabolic pool depletion have lead to speculation that restoring $CR_{tot}$ and TAN to normal levels may represent an alternative and/or complementary strategy for therapeutic intervention in the failing heart (5).

Putative metabolic therapy may be explored on the basis of our simulation of cardiac energetics in hypertrophic remodeling. Fig. 3 illustrates the impact of increasing the creatine pool. Here model-predicted $\Delta G_{ATPase}$ at maximal work rate is plotted as a function of LVW/BW and $CR_{tot}$, where TEP and TAN are set at their values as functions of LVW/BW determined above from the canine LVH data. The model predicts that as LVW/BW increases the optimal $CR_{tot}$ decreases (given prescribed values of TAN and TEP) and that significant changes in either direction will lead to altered cardiac energetic state. Furthermore, increases in $CR_{tot}$ above levels observed in LVH are predicted to deteriorate the energy state. Thus the experimentally observed decrease in the creatine pool helps the heart to maintain its energetic state close to normal during the adaptive stage of hypertrophic remodeling.

These model predictions are consistent with the findings of Neubauer et al. (14) and Wallis et al. (15), who investigated the effects of increasing creatine transporter activity in transgenic mice and report that an increase of $CR_{tot}$ of up to 4-fold compared with normal results in LV dilation, hypertrophy, and mechanical dysfunction (15). These results imply that manipulating $CR_{tot}$ without simultaneous changes in other metabolic pools may not be an effective intervention for the failing heart. In other words, as illustrated in Fig. 2, the pools of $CR_{tot}$, TEP, and TAN are well balanced with respect to one another even during hypertrophic remodeling. Beneficial metabolic therapy will depend on elevating the 3 pools simultaneously by reversing the evolution pathway illustrated in Fig. 2D.

**Possible Metabolic Signals Influencing Remodeling.** Our findings that the cytoplasmic ATP hydrolysis potential in the early and moderate LVH heart may remain at a near-normal level are

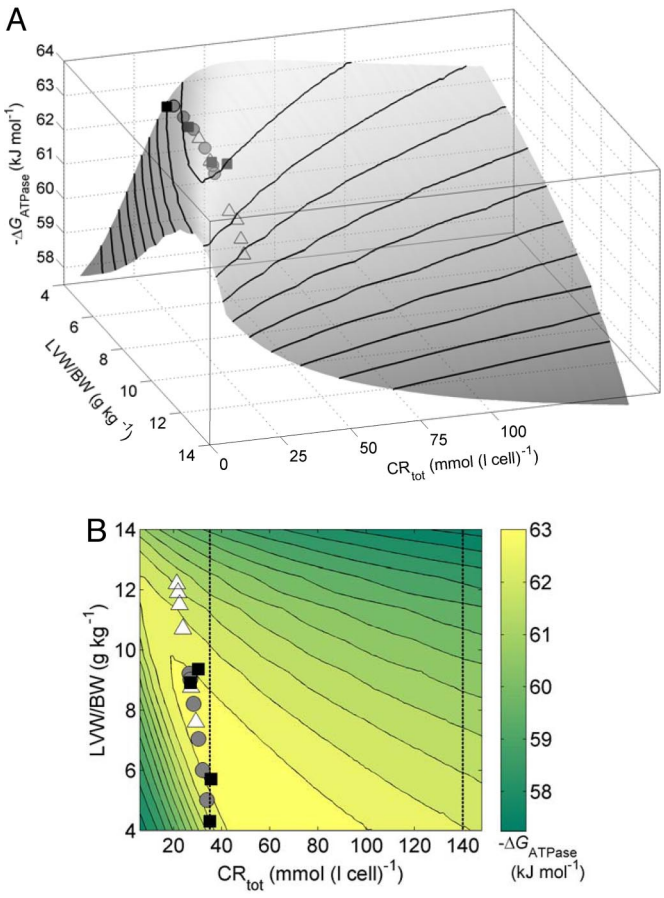


**Fig. 3.** Effects of $CR_{tot}$ on the cardiac energetic state in LVH. Model-predicted ATP hydrolysis potential $\Delta G_{ATPase}$ at maximal $MVO_2$ is plotted as a function of $CR_{tot}$ and LVW/BW. For each value of LVW/BW, the TEP and TAN pools are fixed at values determined for the analysis illustrated in Fig. 2. Data points for LVH canine heart are plotted using the symbols defined in the legend of Fig. 2. The same results are illustrated as a surface projection (*A*) and a contour plot (*B*). The vertical lines in *B* indicate the normal baseline $CR_{tot}$ and a 4-fold increase over normal.

associated with decreased $[Pi]_c$ and increased $[ADP]_c$. Experimental observation shows that the mitochondrial oxidative capacity is not reduced despite the significant changes in phosphate metabolite levels and mitochondrial oxidative phosphorylation protein expressions in the failing heart (6, 16). This seeming inconsistency between largely conserved oxidative capacity in the LVH heart and energy starvation in the CHF heart may be partially explained by the 2 stages of cardiac evolution during the development of the failing heart. Our computational analysis does not predict what specific signaling and proteomic changes occur during LVH remodeling. However, it does give insight into potential mechanisms driving remodeling that may be driven by in part by metabolic changes through signaling pathways modulated by cardiac AMP levels, reactive oxygen species, and other metabolites. Fig. 4 plots model predictions of cytoplasmic [AMP] and mitochondrial $QH_2$ associated with metabolic remodeling in LVH. We see that [AMP] is predicted to vary from below the apparent half-maximal activation of cardiac AMP-activated protein kinase (17), to above the activation level for LVW/BW at the critical transition point and higher. Similarly, mitochondrial $QH_2$, which represents an important redox donor for generation of oxygen radicals (18), is predicted to increase in proportion to LVW/BW. Thus, although our model necessarily

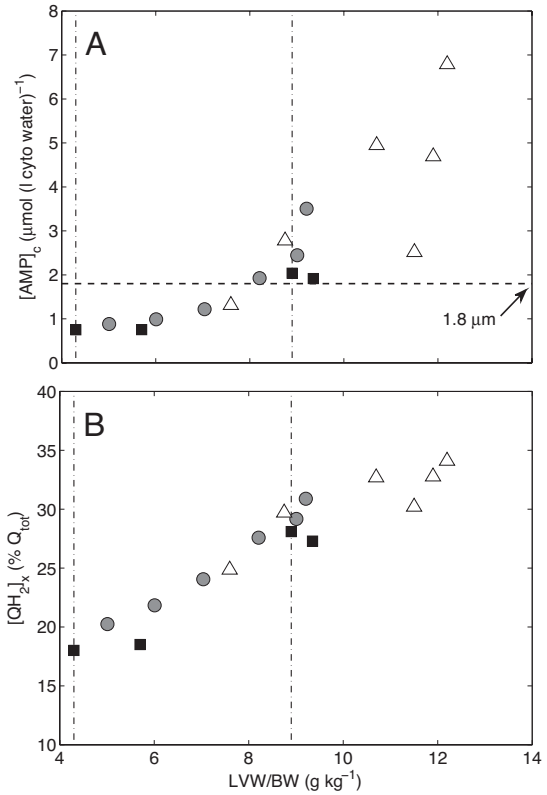


**Fig. 4.** Changes of cytosolic AMP concentration ($[AMP]_c$) and faction of mitochondrial ubiquinol during evolution to heart failure. (*A*) $[AMP]_c$ is plotted against LVH severity (LVW/BW). The symbols and 2 dot-dash vertical lines are defined as in Fig. 2 *A* and *B*. The horizontal dashed line represents the apparent AMP concentration at half-maximal activation of cardiac AMP-activated protein kinase (17). (*B*) The predicted reduced faction of mitochondrial ubiquinol ($[QH_2]_x/Q_{tot}$) is plotted vs. LVW/BW.

provides a simplified representation of the manifold biochemical changes associated with LVH (4), it does suggest that the observed reduction in metabolic pools may activate downstream pathways associated with both AMP-activated protein kinase and oxidative stress.

**Summary.** In summary, this theoretical/computational study reveals that there is a critical phenomenon associated with changing metabolic function in heart disease, whereby a drastic drop in the energy state of the heart occurs when certain metabolic variables change past a critical tipping point. Steady progressive reduction in of TEP, $CR_{tot}$, and TAN is associated with a tipping point in $\Delta G_{ATPase}$ at LVW/BW = ≈9 g heart/(kg body), as shown in Fig. 2*B*. The associated model predictions are coincident with several experimentally observed phenomena: (*i*) the predicted metabolic tipping point coincides with the transition to severe cardiac dysfunction indicated by end-diastolic pressures greater than 15 mmHg in dogs (6, 8); (*ii*) the tipping point is associated with a ≈30% reduction of TAN reduction (Fig. 2*D*), consistent with observations in humans in heart failure (3); (*iii*) the predicted cytoplasmic AMP at the tipping point is ≈1.6 mM and equal to the apparent AMP concentration at half-maximal activation of cardiac AMP-activated protein kinase (17); (*iv*) oxidative stress in the myocardium is predicted to progressively increase as the metabolic pools are diminished; and (*v*) at given values of TAN and TEP during hypertrophic remodeling, $CR_{tot}$ attains a value that is associated with optimal $\Delta G_{ATPase}$. Thus, both increases and decreases to the creatine pool are predicted to result in diminished energetic state unless accompanied by appropriate simultaneous changes in the other pools.

Wallis et al. (15) postulate that the creatine and phosphate pools are maintained in a ''fine balance'' in the healthy heart. Our findings indicate that the fine balance between the 3 metabolic pools studied here is maintained during hypertrophic remodeling, even though the absolute pools sizes are shrinking. The model prediction that the observed decrease in the creatine pool during hypertrophic remodeling is adaptive and actually helps to preserve the energetic state of the heart is perhaps controversial and requires further experimental investigation.

## Materials and Methods

**Calculation of Metabolite Pools.** The definitions of $CR_{tot}$, TEP, and TAN are given in Eqs. **1**, **2**, and **3**, respectively.

$$CR_{tot} = V_{cyto}W_c([CrP]_c + [Cr]_c), \quad [1]$$

$$\begin{aligned} TEP = {} & V_{cyto}W_c(2[ATP]_c + [ADP]_c + [Pi]_c + [CrP]_c) \\ & + V_{mito}W_i(2[ATP]_i + [ADP]_i + [Pi]_i + [CrP]_i) \\ & + V_{mito}W_x([ATP]_x + [Pi]_x + [GTP]_x), \end{aligned} \quad [2]$$

$$\begin{aligned} TAN = {} & V_{cyto}W_c([ATP]_c + [ADP]_c + [AMP]_c) \\ & + V_{mito}W_i([ATP]_i + [ADP]_i + [AMP]_i) \\ & + V_{mito}W_x([ATP]_x + [ADP]_x). \end{aligned} \quad [3]$$

Here the subscripts ''x,'' ''i,'' and ''c'' denote matrix, intermembrane, and cytoplasmic (extramitochondrial) spaces, respectively. For example, $[ATP]_x$ denotes matrix ATP concentration, whereas $[ATP]_c$ denotes ATP concentration in the cytoplasm. The parameters $V_{cyto}$ and $V_{mito}$ are cellular volume of cytoplasm and mitochondria, respectively; $W_c$, $W_i$, and $W_x$ are water fractions in cytoplasm, mitochondrial intermembrane space, and mitochondrial matrix, respectively. These values are computed according to the myocardial density and composition of the rat heart reported by Vinnakota and Bassingthwaighte (19) and listed in *SI Appendix*, Table S2.

**Computational Model.** The model is mathematically described by using the differential equations listed in the *SI Appendix* of this work and appendixes of our previously published work (2, 20), which also describe details on model parameterization and validation.

**Experimental Data.** All experimental data used in this study are collected from the sources detailed in the text.

**ACKNOWLEDGMENTS.** This work was supported by National Institutes of Health Grants HL072011 (to D.A.B.), HL50470 (to J.Z.), and HL67828 (to J.Z.).

1. Balaban RS (1990) Regulation of oxidative phosphorylation in the mammalian cell. *Am J Physiol* 258(3 Pt 1):C377–C389.
2. Wu F, Zhang EY, Zhang J, Bache RJ, Beard DA (2008) Phosphate metabolite concentrations and ATP hydrolysis potential in normal and ischaemic hearts. *J Physiol* 586(Pt 17):4193–4208.
3. Ingwall JS, Weiss RG (2004) Is the failing heart energy starved? On using chemical energy to support cardiac function. *Circ Res* 95:135–145.
4. Ingwall JS (2009) Energy metabolism in heart failure and remodelling. *Cardiovasc Res* 81:412–419.
5. Neubauer S (2007) The failing heart—an engine out of fuel. *N Engl J Med* 356:1140–1151.
6. Bache RJ, et al. (1999) Myocardial oxygenation at high workstates in hearts with left ventricular hypertrophy. *Cardiovasc Res* 42:616–626.
7. Bache RJ, et al. (1994) High-energy phosphate responses to tachycardia and inotropic stimulation in left ventricular hypertrophy. *Am J Physiol* 266(5 Pt 2):H1959–H1970.
8. Zhang J, et al. (1993) Bioenergetic abnormalities associated with severe left ventricular hypertrophy. *J Clin Invest* 92:993–1003.
9. Ye Y, Gong G, Ochiai K, Liu J, Zhang J (2001) High-energy phosphate metabolism and creatine kinase in failing hearts: A new porcine model. *Circulation* 103:1570–1576.
10. Ingwall JS, et al. (1985) The creatine kinase system in normal and diseased human myocardium. *N Engl J Med* 313:1050–1054.

11. Smith CS, Bottomley PA, Schulman SP, Gerstenblith G, Weiss RG (2006) Altered creatine kinase adenosine triphosphate kinetics in failing hypertrophied human myocardium. *Circulation* 114:1151–1158.
12. Weiss RG, Gerstenblith G, Bottomley PA (2005) ATP flux through creatine kinase in the normal, stressed, and failing human heart. *Proc Natl Acad Sci USA* 102:808–813.
13. Masri C, Chandrashekhar Y (2008) Apoptosis: A potentially reversible, meta-stable state of the heart. *Heart Fail Rev* 13:175–179.
14. Neubauer S, et al. (1999) Downregulation of the Na(+)-creatine cotransporter in failing human myocardium and in experimental heart failure. *Circulation* 100:1847–1850.
15. Wallis J, et al. (2005) Supranormal myocardial creatine and phosphocreatine concentrations lead to cardiac hypertrophy and heart failure: Insights from creatine transporter-overexpressing transgenic mice. *Circulation* 112:3131–3139.
16. Gong G, et al. (2003) Oxidative capacity in failing hearts. *Am J Physiol Heart Circ Physiol* 285:H541–H548.
17. Frederich M, Balschi JA (2002) The relationship between AMP-activated protein kinase activity and AMP concentration in the isolated perfused rat heart. *J Biol Chem* 277:1928–1932.
18. Turrens JF (2003) Mitochondrial formation of reactive oxygen species. *J Physiol* 552(Pt 2):335–344.
19. Vinnakota KC, Bassingthwaighte JB (2004) Myocardial density and composition: A basis for calculating intracellular metabolite concentrations. *Am J Physiol Heart Circ Physiol* 286:H1742–H1749.
20. Wu F, Yang F, Vinnakota KC, Beard DA (2007) Computer modeling of mitochondrial tricarboxylic acid cycle, oxidative phosphorylation, metabolite transport, and electrophysiology. *J Biol Chem* 282:24525–24537.
21. Zhang J, et al. (2005) Nitric oxide regulation of myocardial O2 consumption and HEP metabolism. *Am J Physiol Heart Circ Physiol* 288:H310–H316.
22. Zhang J, From AH, Ugurbil K, Bache RJ (2003) Myocardial oxygenation and high-energy phosphate levels during KATP channel blockade. *Am J Physiol Heart Circ Physiol* 285:H1420–H1427.
23. Ochiai K, et al. (2001) Effects of augmented delivery of pyruvate on myocardial high-energy phosphate metabolism at high workstate. *Am J Physiol Heart Circ Physiol* 281:H1823–H1832.
24. Gong G, Ugurbil K, Zhang J (1999) Transmural metabolic heterogeneity at high cardiac work states. *Am J Physiol* 277(1 Pt 2):H236–H242.